PAPER • OPEN ACCESS

The influence of variability on fire weather conditions in high latitude regions under present and future global warming

To cite this article: Marianne T Lund *et al* 2023 *Environ. Res. Commun.* **5** 065016

Environmental Research Communications

PAPER

The influence of variability on fire weather conditions in high latitude regions under present and future global warming

Marianne T Lund[1,*], **Kalle Nordling**[1], **Astrid B Gjelsvik**[2] and **Bjørn H Samset**[1]

[1] CICERO Center for International Climate Research, Oslo, Norway
[2] Department of Geosciences, University of Oslo, Norway
* Author to whom any correspondence should be addressed.

E-mail: m.t.lund@cicero.oslo.no

Keywords: fire weather, boreal forests, global warming, climate variability, large ensembles

Supplementary material for this article is available online

OPEN ACCESS

RECEIVED
12 January 2023

REVISED
2 May 2023

ACCEPTED FOR PUBLICATION
19 June 2023

PUBLISHED
28 June 2023

Abstract

Recent years have seen unprecedented fire activity at high latitudes and knowledge of future wildfire risk is key for adaptation and risk management. Here we present a systematic characterization of the probability distributions (PDFs) of fire weather conditions, and how it arises from underlying meteorological drivers of change, in five boreal forest regions, for pre-industrial conditions and different global warming levels. Using initial condition ensembles from two global climate models to characterize regional variability, we quantify the PDFs of daily maximum surface air temperature (SAT_{max}), precipitation, wind, and minimum relative humidity (RH_{min}), and their evolution with global temperature. The resulting aggregate change in fire risk is quantified using the Canadian Fire Weather Index (FWI). In all regions we find increases in both means and upper tails of the FWI distribution, and a widening suggesting increased variability. The main underlying drivers are the projected increase in mean daily SAT_{max} and decline in RH_{min}, marked already at +1 and +2 °C global warming. The largest changes occur in Canada, where we estimate a doubling of days with moderate-or-higher FWI between +1 °C and +4 °C global warming, and the smallest in Alaska. While both models exhibit the same general features of change with warming, differences in magnitude of the shifts exist, particularly for RH_{min}, where the bias compared to reanalysis is also largest. Given its importance for the FWI, RH_{min} evolution is identified as an area in need of further research. While occurrence and severity of wildfires ultimately depend also on factors such as ignition and fuel, we show how improved knowledge of meteorological conditions conducive to high wildfire risk, already changing across the high latitudes, can be used as a first indication of near-term changes. Our results confirm that continued global warming can rapidly push boreal forest regions into increasingly unfamiliar fire weather regimes.

Introduction

Wildfire is an integral natural process in the terrestrial ecosystem, shaping landscapes, influencing ecosystem development and composition, and regulating biogeochemical cycles (Screen *et al* 2015, Pausas and Keeley 2019). Wildfires also result in land cover changes and large emissions of carbon dioxide and air pollutants that have consequences for the local surface energy balance, climate air quality and other quantities (Rocha and Shaver 2011, Liu *et al* 2014, Reid *et al* 2016), and they can have devastating socioeconomic consequences when occurring near populated regions (UNEP Spreading like Wildfire 2022). Knowledge of how fire risk and fire regimes may change around the world in a future warmer climate is therefore a key prerequisite for adaptation and disaster risk management (Jones *et al* 2022).

Wildfire occurrence and severity is a result of the complex interplay between natural factors, such as fuel availability and lightning, and anthropogenic influence, such as land management practices or ignition

(Flannigan *et al* 2009). However, meteorological conditions present a key underlying risk factor. Conditions conducive to high wildfire risk are characterized by the combination of high temperatures, little precipitation and low humidity, and often high winds—weather variables that are all affected by global warming. Evidence is emerging that human-induced climate change is already promoting an increase in the frequency of the high-risk fire weather and duration of the fire season in several regions (Jolly *et al* 2015, Abatzoglou *et al* 2019, Jones *et al* 2020). While studies indicate that the global burnt area has been declining over the past couple of decades, driven by less savannah and grassland burning in Africa, Australia, and Central America (Doerr and Santín 2016, Lizundia-Loiola *et al* 2020), fire activity is rising in many areas. However, many global models still struggle to reproduce observed regional and seasonal trends and patterns in burnt area, and have known issues with fire modelling in general (Hantson *et al* 2020, Jones *et al* 2022).

Here we focus on one region that has seen major recent changes, the high (>60°N) northern latitudes, that includes large areas of boreal forests. Recent years have seen unprecedented fire activity and shift in fire regimes in the pan-Arctic region (York *et al* 2020, McCarty *et al* 2021), leading to severe consequences including unhealthy air quality in towns and cities (Shaposhnikov *et al* 2014, Woo *et al* 2020). Concurrently, the region has warmed much more rapidly than the global mean, leading to substantial environmental and climatic changes, including changes in extreme events (Walsh *et al* 2020), many of which in turn interact with wildfire risk. For instance, studies have found an increase in lightning activity in the Arctic (Holzworth *et al* 2021, Chen *et al* 2021b), the dominant fire ignition source in the region (Kasischke and Turetsky 2006, Veraverbeke *et al* 2017). Other have suggested that increasingly hot summers may not only be driving more fires in that season but may also be fueling an increase in so-called overwintering fires in the boreal region (McCarty *et al* 2020, Scholten *et al* 2021, Xu *et al* 2022).

While the body of literature on high-latitude wildfire is growing, studies often focus on individual regions, fire types, or processes, and have different methodological frameworks, scenarios, and metrics. For instance, Flannigan *et al* (2009) found that 75% of papers on wildfire and climate focused on North America, while Walsh *et al* (2020) recently noted that studies of extreme weather in the northern areas are largely uncoordinated and have historically been limited. Furthermore, human-induced effects on weather and climate not only manifest as shifts in the means and extremes of the variables but can also change the shapes of their distributions. Comprehensive understanding of climate risk therefore involves quantification of the full, regional Probability Density Functions (PDFs) of the local meteorological conditions that contribute to fire risk. These contain information on expected weather not apparent from the distribution mean or tails, but through changes to their overall shape. While this type of information has historically not been available from simulations with Earth System Models (ESMs), the advent of the large initial condition ensembles of coupled climate model simulations has opened new opportunities for studying climate variability and how it evolves with global warming (e.g. Samset *et al* 2019, Deser *et al* 2020, Maher *et al* 2021, van der Wiel and Bintanja 2021).

In the present analysis, we leverage the power of two such large ensembles. Our aim is to provide a detailed and systematic characterization of the distribution and variability of weather variables relevant for high risk of wildfire, and the projected evolution with global warming in current ESMs and scenarios, across the boreal high latitude regions. Our core assumption is that even if fire modelling overall is still a challenge in global models, there are robust relationships between fire risk and the evolution of underlying meteorological variables, and that quantifying how these change under global warming therefore gives additional information on near-term conditions for elevated fire risk. A secondary objective is to develop and document a flexible framework that can easily be extended to further variables, datasets, and research questions. Using data from two global ESMs, we therefore consistently quantify the seasonally resolved PDFs of daily climate data in five high-latitude regions in North America, Scandinavia, and Russia (figure 1(a)), for preindustrial conditions and four levels of global warming, and show how they combine into a commonly used overall index for fire weather. Our analysis provides a comprehensive picture of projected changes in key meteorological drivers of fire risk at high latitudes, showing both that future changes in weather-related fire risk are heterogeneous in magnitude across boreal regions, and that large ensemble modelling techniques can provide comprehensive, user-oriented information for mitigation and adaptation.

Methods

Building on methodology developed by Samset *et al* (2019), we quantify the PDFs of daily mean and maximum near-surface (2-meter) air temperature (SAT and SAT_{max}), precipitation (precip), minimum daily surface relative humidity (RH_{min}), and surface wind speed (wind). While other climatic and weather-related factors, such as soil moisture and snow, also influence wildfire regimes, we focus on the variables that pose the most direct risk factors and form the basis for the Canadian forest fire weather index (see below), which we use as an aggregate measure of the change in wildfire risk.

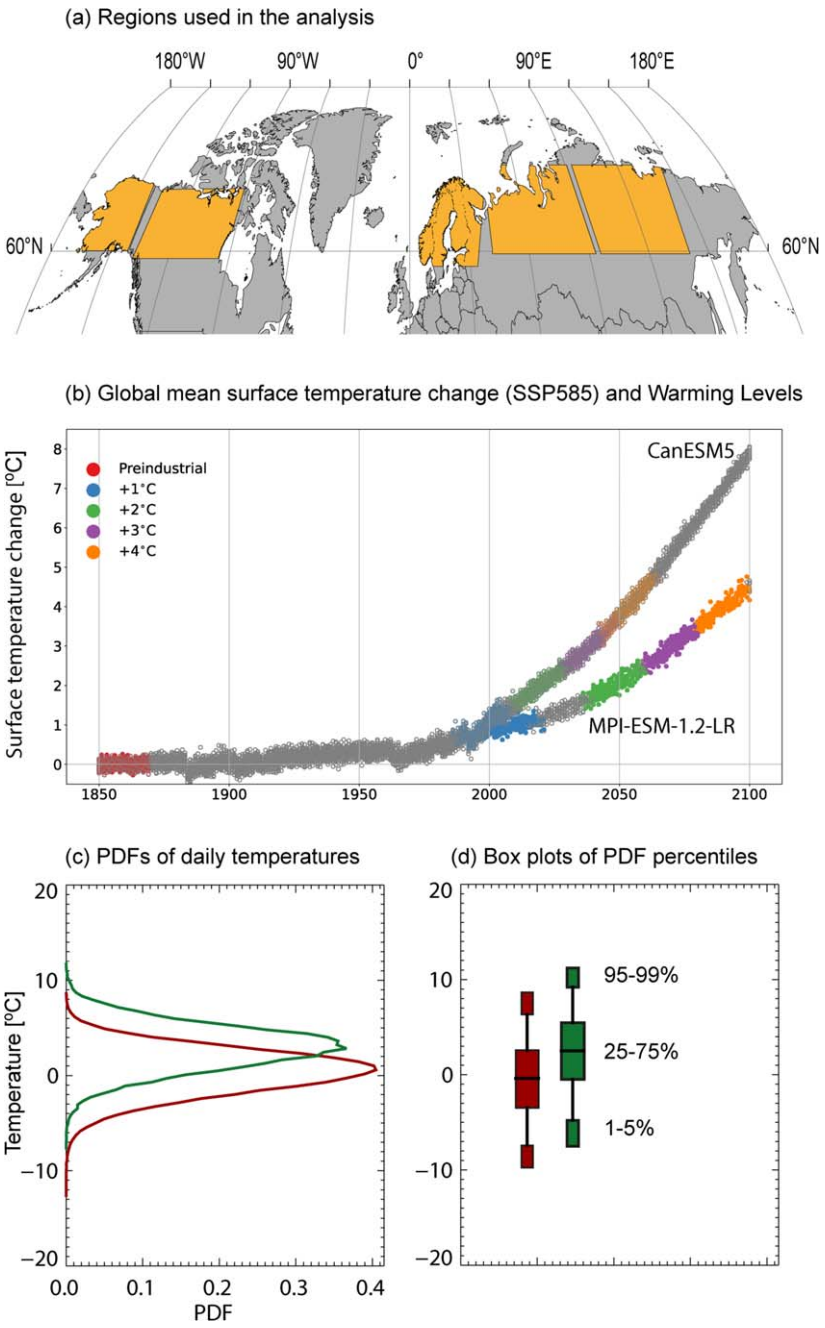

Figure 1. Methodology: (a) Geographical definition of the regions considered in the analysis. (b) Global, annual mean surface temperature for each year in the MPI-ESM1–2-LR and CanESM5 ensembles. Colors shows data in each warming level. (c) Illustrative example of PDFs for daily mean temperature in 1850–1900 climate and under +2 °C of global warming. (d) same as (c) but shown as the box plots used for comparison of the results of our analysis.

The initial condition ensemble chosen for our primary analysis is that from the MPI-ESM1-2-LR (Mauritsen *et al* 2019), produced for ScenarioMIP as part of the sixth phase of the Coupled Model Intercomparison Project (CMIP6) (O'Neill *et al* 2016). The MPI-ESM1-2-LR has an Equilibrium Climate Sensitivity (ECS) of 2.77 K (Zelinka *et al* 2020), close to best estimate assessed by the Intergovernmental Panel on Climate Change (IPCC) (Forster *et al* 2021) and the grand ensemble from the same model using the previous generation climate scenarios (Maher *et al* 2019) has been extensively used in studies of climate variability. Ensembles from several other models are becoming available. While a comprehensive multi-model analysis is beyond the scope of the present study, we also include the ensemble from CanESM5 (Swart *et al* 2019). In contrast to MPI-ESM1-2-LR, CanESM5 has a high (5.6 K) ECS and is therefore used as a sensitivity case and first order investigation of model dependence of our findings. The MPI-ESM1-2-LR and CanESM5 ensembles consist of 10 and 25 members, respectively, forced with historical emission data for 1850–2014 and Shared Socioeconomic Pathway 5–8.5 (SSP585) emissions for 2015–2100 (Feng *et al* 2020). To investigate potential scenario dependence of the climate

under a given global warming level, we also use a corresponding ensemble forced with SSP126 emissions (see Supplementary Information). To validate the skill of the two models in simulating PDFs of daily weather under present day conditions, we compare to daily ERA-5 reanalysis data from 2000–2020 (Hersbach *et al* 2020, Hersbach *et al* 2018).

Our method for calculating PDFs is illustrated in figure 1. They are calculated on a monthly basis for five regions (Alaska, Canada, Fennoscandia, East Siberia, and West Siberia—figure 1(a)), for the 1850–1900 period (i.e. preindustrial conditions), and for +1 °C, +2 °C, +3 °C and +4 °C of global surface temperature change (i.e. global warming levels, GWLs). Using GWLs in projections of climate hazards and impacts, rather than being restricted to a given emission scenario, has been increasingly adopted in the scientific literature, including the sixth Assessment Report by the Intergovernmental Panel on Climate Change (Chen *et al* 2021a).

Selection of GWL follows the approach from Lee *et al* (2021). We first calculate the global, annual mean surface temperature for all years in the ensemble (figure 1(b)). Next, we identify the first year when the 20-year running mean hits the respective GWL and select data from all years in the ± 10-year range surrounding this. For each warming level we then calculate seasonal, regionally (land-only) averaged PDFs of daily data for each of the variables listed above, as illustrated in figure 1(c) for temperature in a preindustrial and +2 °C world. We note that the number of grid points used in the averaging vary between regions, and between ESMs (due to different resolutions) (table S1).

Results are also presented as box plots of the PDF percentiles to facilitate better comparison across both regions and GWLs (figure 1(d)). Finally, to synthesize how the PDFs evolve with warming, in terms of both shape and mean, we summarize the change in width (i.e. standard deviation) and overlap of the PDF between each GWL and the 1850–1900 period. Change in overlap, referred to as overlap displacement, is calculated as in Samset *et al* (2019): we quantify the area of overlap (AoO) between two PDFs and plot (1-AoO)*100. The result is a number between 0 and 100%, where 100% indicate that the PDF has shifted entirely from the 1850–1900 baseline.

To explore the aggregate change in distribution and variability of weather-related fire risk, we use the Canadian forest fire weather index (FWI). Developed in the 1970s (Van Wagner 1987), the Canadian FWI system provides a numerical rating of fire potential and is used in forecasts of fire danger by e.g. the Canadian Wildland Fire Information System. The source code is avaialable from Wang *et al* (2015). The FWI model is based exclusively on input of meteorological data (temperature, precipitation, relative humidity, and wind) and consists of six components that account for the effects of fuel moisture on fire behavior. The algorithm is based on a single standard fuel type that be described as a generalized pine forest. The resulting FWI combines indices for initial fire spread and fire buildup and is a unitless value expressing general fire intensity potential. We apply a definition of fire season based solely on temperature in our FWI calculations, i.e. the season is assumed to start when there are three consecutive days with maximum temperature exceeding +12 °C and, conversely, end after three consecutive days of temperature below +12 °C. When this criterion is fulfilled, we calculated the daily FWI for each grid point and quantify the corresponding regionally averaged PDFs for each GWL. Qualitative levels of fire risk follow Giannakopoulos *et al* (2020): very low < 2, low = 5–11, moderate = 11–21, high = 21–38, very high = 38–50. Finally, to investigate the sensitivity of the FWI to changes in individual meteorological variables, we also perform additional calculations where one and one variable is changed back from the value under +4 °C GWL to its 1850–1900 condition.

Results

We first present the evolution of the regional distributions of individual meteorological variables with GWL, then discuss projected changes in the FWI. We focus on the boreal summer (JJA) when the wildfire season is at its peak, but also discuss spring and fall distributions. The performance of our chosen ESMs in reproducing current conditions is presented in Sect. S1. Briefly, both models agree reasonably well with ERA5 reanalysis, with the best agreement for SAT, $SAT_{max,}$ and wind, and the largest biases for RH_{min}.

Variability and evolution of individual meteorological variables with global warming

Figure 2 shows box plots of the JJA area-average PDFs of daily temperature, precipitation, relative humidity, and wind from the MPI-ESM1–2-LR. Consistent with global climate warming, we find increasing daily SAT (not shown) and SAT_{max} across all regions. Changes are notable already at +1 °C global warming relative to 1850–1900, where for instance the average of the daily SAT_{max} PDF in Canada is already outside the 25–75 percentile range of the 1850–1900 climate in this model, as well as between +1 °C and +2 °C. At the +4 °C GWL, we find that the regional mean of both SAT and SAT_{max} increase by 4 °C–5 °C. This is of the same order of magnitude as changes projected for the end of the century under the RCP8.5 scenario (Collins *et al* 2013). The precip PDFs show smaller shifts in mean, but a marked widening of the distributions is found for most GWLs

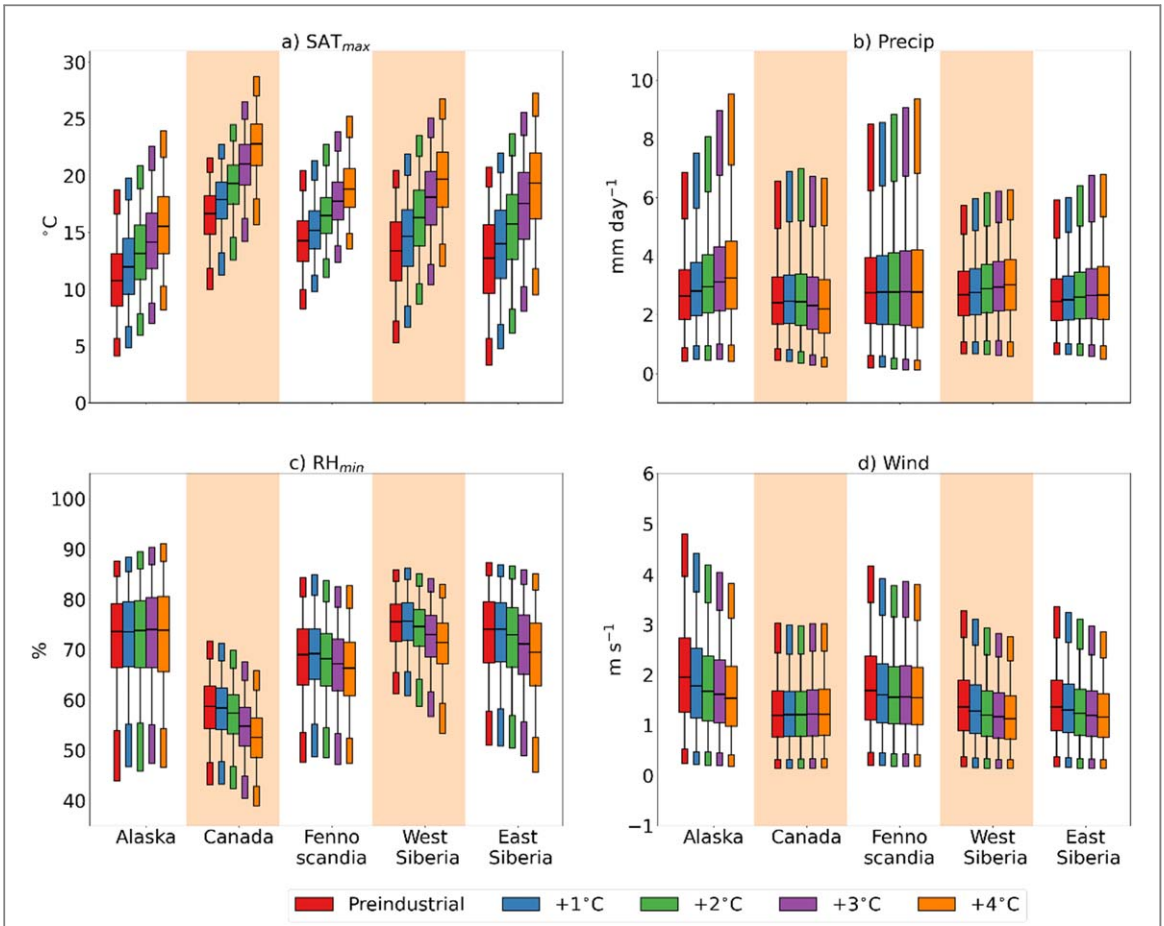

Figure 2. Evolution of PDFs with global warming for MPI-ESM1–2-LR: Box plots of the PDFs of regional daily (a) maximum surface air temperature, (b) precipitation, (c) minimum surface relative humidity, and (d) wind in boreal summer (JJA), as projected for different global GWLs.

and regions. In Alaska and West Siberia there is a projected increase in the mean of the precipitation distribution with global warming, while the Fennoscandia distribution mean changes little and there is a decrease in mean daily precipitation for the two highest warming levels in Canada. An increase in precipitation could seemingly be an offsetting factor for wildfire risk. However, a well-established consequence of global warming is that much of the expected increase in precipitation manifests as more extreme, short-duration precipitation events (Fischer and Knutti 2016). This is also evident from the increase in the upper 5th percentile of our PDFs, particularly in Alaska and Fennoscandia. We note that may be local variations within regions. We also find a reduction in mean daily RH_{min} in all regions except Alaska for GWL of 2 °C to 4 °C. Moreover, the RH_{min} declines relatively linearly with increasing SAT_{max}, at least within the ranges covered in this dataset, for all regions and GWLs, further supporting that the summertime warming can be associated with periods of drying despite the increase in precipitation. Finally, for wind we find a general decrease in the mean and upper tail of the distributions with warming in the MPI-ESM1–2-LR, except for Fennoscandia where there is little change. Increased daily surface air temperature and reduced minimum relative humidity at the surface are key indicators of high likelihood of wildfire occurrence. The combined effect of changes in the meteorological variables on, as well as their relative contributions to, the distribution and evolution of the FWI is discussed below.

Figure 3 provides further overview and details of the distributional changes with warming across variable, region, and GWL. Here we summarize the change in mean and standard deviation (SD) relative to the 1850–1900 distribution, as well as the overlap displacement (see Methods). Firstly, the blue and red color indicates shifts of the PDF mean to the left (lower values) or right (higher values) of the 1850–1900 mean, respectively. Secondly, the concurrent narrowing (i.e. decreasing SD) or widening (increase in SD) of the distributions is marked by hatched or blank boxes. That is, if a box is hatched, the distribution of the respective variable shows less variability than the 1850–1990 baseline. Finally, the strength of the color of the boxes illustrates how far away from the 1850–1900 baseline the given regional PDF has shifted. The darker the color, the less the pre-industrial and future projected distributions overlap, with direction of displacement indicated by the blue and red. A value of 100% indicate that there is no longer any overlap between the 'new climate' and the 1850–1900 distribution. Numerical values are provided in table S2. Such shifts in expected variability are an

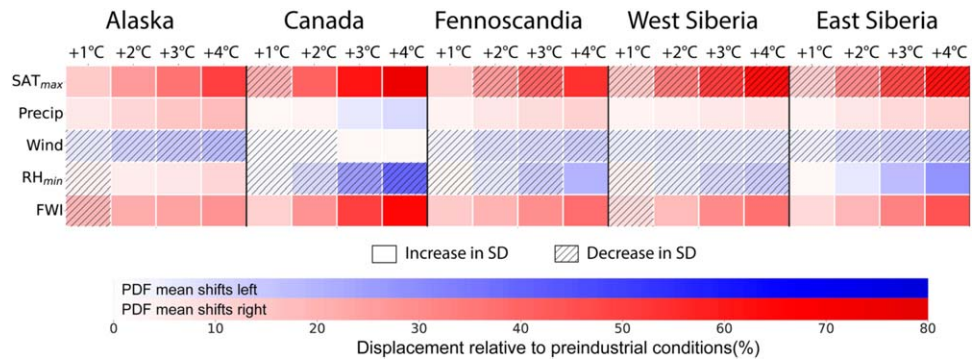

Figure 3. Summary of PDF changes in MPI-ESM1–2-LR: Synthesis of change in mean, width and overlap displacement relative to 1850–1900 for each region, variable, and GWL. Hatching shows where the standard deviation of the PDF decreases, i.e. the distribution narrows, while boxes without hatching shows a widening of the distribution. The color indicates a shift in mean to the left or right of the 1850–1900 mean, while the color scale shows increasing overlap displacements, where 100% indicate that there is no longer any overlap between the 'new climate' and the 1850–1900 distribution.

important consideration for climate risk, as larger displacement implies increasingly unfamiliar (for society) climates.

As an example of how to read the figure, consider first SAT_{max}. Across all regions, the mean of the PDF shifts to the right of the pre-industrial baseline, i.e. towards higher temperatures, as was already seen in figure 2. The distributions of SAT_{max} are shifted substantially beyond the 1850–1900 distribution already at +2 °C global warming and are projected to be displaced by 50% or more by +4 °C for all regions. The change in shape of the distributions is, however, more variable across region, with West and East Siberia projected to experience less variability in SAT_{max} for all GWLs but the opposite for Alaska.

Also seen is the narrowing of the wind PDF across all regions and almost all GWLs, as well as the consistent widening of the precipitation distribution. For RH_{min}, there is, similarly to SAT_{max}, more regional heterogeneity in the change of shape. However, we note that there is no consistent pattern of shape changes between SAT_{max} and RH_{min} in a given region. In Alaska and East Siberia, the model projects more variability (increased standard) for all GWLs, while Canada and West Siberia are projected to experience less variability with global warming relative to the pre-industrial baseline. For Fennoscandia, a decrease in the standard deviation is found up until +3 °C.

The daily distributions of all variables analyzed are projected, and have in many cases already started, to shift away from the 1850–1900 state with global warming, but to different degrees and with geographical variations. The daily PDFs of precipitation and wind show the smallest overlap displacements with warming. This is partly due to smaller shifts in the mean and partly due to the larger intrinsic variability. In contrast, the distributions of SAT_{max} are shifted substantially beyond the 1850–1900 distribution already at +2 °C global warming and are projected to be displaced by more than 50% by +4 °C. We note that while the regional overlap displacements are similar in magnitude for a +1 °C global warming, differences between boreal regions become more pronounced with subsequent GWLs. In particular, Canada stands out in the case of SAT_{max} and RH_{min}, reflecting both the substantial changes in the mean of the distributions, as well as the narrower baseline PDFs (figure 2).

Changes during spring and fall may also affect fire risk and length of the fire season. Overall, we find the same general details of changes in the regional PDFs during April, May, and September as for summer (not shown). For SAT and SAT_{max}, there is a marked narrowing of the distributions in April and May for most regions and GWLs following loss of the coldest days.

Aggregate changes in fire weather with global warming

Figure 4(a) shows the distribution of the daily FWI and its evolution with GWL. In the high-latitude regions studied here, the summertime distribution is skewed, with a mean generally in the lower-risk values but long tails towards the moderate and high risk (see Methods for definition). The change with GWL is also most evident in upper 5th percentiles. Canada not only has the highest average FWI and widest distribution under current conditions but is also projected to experience the largest increase in both mean and variability with warming, followed by East Siberia. In contrast, the upper 95–99 percentile of daily FWI in Alaska remains in the low FWI interval. For all regions, but most significantly for Canada, the distribution of daily FWI shifts substantially away from its 1850–1900 baseline with global warming (figure 3).

The PDFs are regional averages over quite large areas and high values does not necessarily imply a high risk everywhere within each region. Such spatial differences are evident from figure 4(b), which shows, for each grid box, the total number of days with FWI above 11 (i.e. moderate or higher risk) for the +1 °C GWL (i.e. present-day

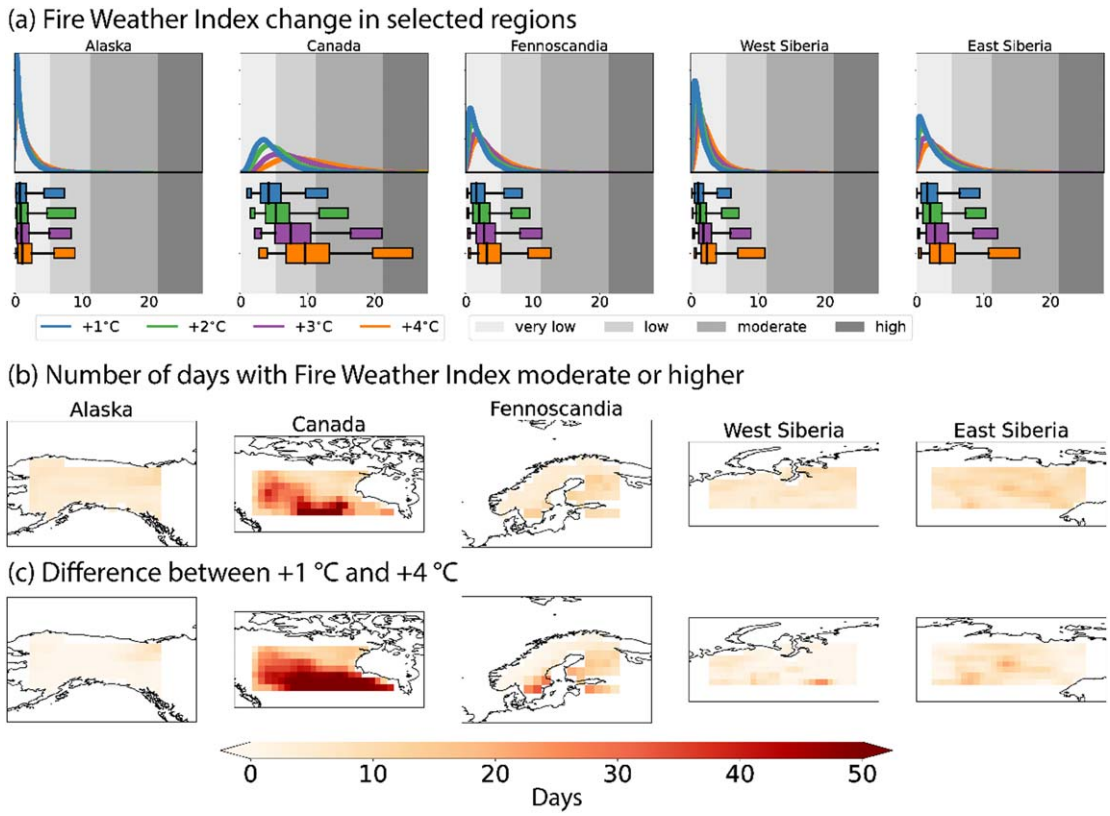

Figure 4. The FWI under global warming: (a) Regional, boreal summer (JJA) PDFs of daily FWI using data from the MPI-ESM1–2-LR. Grey shading indicates qualitative levels of fire risk. (b) Number of days per year when the FWI is 11 or higher (i.e. moderate or higher risk) for the +1 °C GWL, and (c) change in the annual total number of days with moderate or higher fire risk between +1 °C and +4 °C GWLs.

climate conditions). For instance, there are more such days in the southern and western domain of our Canadian region, and more days in Finland and southern Sweden than in Norway. However, for all regions, the number of moderate or higher FWI days increases with global warming (figure 4(c)). For Canada and Fennoscandia, we estimate that the regional mean number of moderate or higher FWI days doubles under +4 °C global warming relative to a +1 °C world. Smaller increases of 20%–60% are found on average for Alaska and Siberia. Spatially, the increase is generally largest where the number of days is currently highest.

By using calculations of FWI where one and one meteorological variable is moved back to the 1850–1900 conditions (see Methods), we find that changes in SAT_{max} and RH_{min} are the dominant drivers of the changes in the FWI distribution across all our regions (figure S4). This is consistent with recent findings by for other wildfire-prone regions (Touma *et al* 2021). The sensitivity to RH_{min} helps to explain the relatively small changes to mean FWI and total number of moderate-to-high FWI days in Alaska, despite the pronounced increase in the mean and upper tail of SAT_{max} also in this region (figure 2). The sensitivity is also evident from the smaller changes in FWI estimated with the CanESM5 (figure S3), which had smaller decreases in mean daily RH_{min} (figure S2) than MPI-ESM-1–2-LR.

Discussion

We have used the Canadian FWI system to assess projected regional changes in weather-related wildfire risk, due to its broad use in our focus regions and the literature, but other indices exist. Different indices and systems have been compared for boreal landscapes in several previous studies, including in Finland (Vajda *et al* 2014), Alaska (Mölders 2010, Ziel *et al* 2020), and Canada (Lee *et al* 2002). We refer to these studies for more detail on the performance but note that the choice of fire weather index could influence our findings. Moreover, as also suggested elsewhere (e.g. Ziel *et al* 2020, Balch *et al* 2022), current indices may not fully capture the climate-induced changes affecting fire danger in the future, such as snow pack and season, early and late season droughts, and diurnal temperature range, or factors relating to peat and overwintering fires which are receiving increased attention also in the Arctic region (Scholten *et al* 2021), warranting further research and development. Our analysis is at present limited to the weather variables most directly related high fire risk and forming the basis for

the FWI. We have, however, established a flexible framework that can easily be applied to other climate and weather indicators or fire danger indices, including but not limited to the abovementioned.

We specifically note that our quantification of FWI does not consider the concurrent presence or changes in variability of snow cover, which could affect results, particularly in spring and fall. A general trend of shorter season, and reduced extent of, terrestrial snow cover, consistent with global warming, has been documented in the northern latitudes, and in particular during the spring months of March and May, albeit with large regional interannual variability (Mudryk *et al* 2020, Walsh *et al* 2020). Moreover, Mudryk *et al* (2020) identified a single linear relationship between snow cover in spring projected by the CMIP6 model and the global SAT changes for the Northern Hemisphere overall, suggesting an 8% decrease in spring snow extent, relative to present-day, per degree of global warming. A shorter snow season is partly driven by the transition from snow to rain and a recent study found that the most recent projections from CMIP6 show that the Arctic may experience a transition from a snow- to a rain-dominated regime in summer and fall much earlier than previously projected (McCrystall *et al* 2021). While that study considered the region north of 70°N, shifts in the hydrological regime can be expected for the regions considered in our analysis as well. As the presence of snow precludes fires, this overall evolution indicates that our FWI based quantifications may underestimate future increases in the boreal regions. Quantifying this underestimate would however require dedicated simulations, that are not available at the present time.

The focus of the present study is to characterize and map projected changes in regional weather-related fire risk, and further work would be required to link these to more specific processes or drivers beyond global warming. For instance, previous studies have linked increasing fire activity in the Western US (Zou *et al* 2021) and high-latitude hot extremes (Screen *et al* 2015) to declining Arctic sea ice. Natural variability has also been found to contribute to increasing weather-related fire risk over the Western US, although to a smaller degree than anthropogenic climate change (Zhuang *et al* 2021). An increasing variability of Arctic sea level pressure with warming has been linked to precipitation variability (Bogerd *et al* 2020). Moreover, the occurrence and severity of fire is dependent on factors not considered here, such as fuel availability, vegetation and landscape changes (e.g. forest management, permafrost thawing, peatland drying), and natural and human ignition sources. See e.g. McCarty *et al* (2021) for an overview of potential ecological transitions relevant for high latitude boreal fire regimes. Furthermore, fire affects the landscape, creating feedback on climate and vegetation. Coupled fire-climate-land use-ecology modeling is an area requiring further efforts by the scientific community (McCarty *et al* 2021). While fire modeling remains challenging, detailed, up-to-date input on how meteorological drivers of fire risk can be expected to change in future can provide first-order information of relevance for stakeholders and communities.

Projections of future climate can exhibit significant spread across ESMs (Lee *et al* 2021). This includes both differences in overall climate sensitivity, which will affect fire changes due to the overall global mean temperature evolution, and in regional climate and the complexity for the processes included. The value of large initial condition ensembles lies in exploring the full influence of internal variability without the presence confounding factors from host model differences, with the caveat that any results will be dependent on the performance of that model. While a multi-ensemble comparison is beyond the scope of our study, we compare the results based on MPI-ESM1–2-LR with those from the CanESM5 for an initial indication of what corresponding results can look like in another host model. Overall, we find similar changes in CanESM5 as in MPI-ESM1–2-LR (figures S2, S3). Although CanESM5 on average is warmer, the changes in SAT_{max} distributions with GWL are similar in both models. For RH_{min}, there are smaller changes in mean compared to MPI-ESM1–2-LR and CanESM is substantially drier in Siberia (figure S2). Due to their different ECS, a given GWL is not reached during the same time period in MPI-ESM1–2-LR and CanESM5, which could in theory contribute to the differences. However, at least for the lower GWLs, we do not find strong evidence of a scenario dependence in either model (section S2). Analyses beyond the current study is needed to better understand inter-model differences.

Our analysis suggests a need for further focus on RH_{min}. RH_{min} is a key driver of changes in the FWI and this is the variable for which we find the most marked model difference and largest biases compared to reanalysis. Of particular interest is a much stronger decrease mean of the RH_{min} PDF for April and May than for JJA in MPI-ESM1–2-LR, in particular in Canada and Fennoscandia. While the springtime variability is also larger, such a drying could be important for early season fire risk, as well as have implications for agriculture. However, there is again substantial model differences. The importance of RH_{min} for the resulting FWI, as well as potentially for other sectors such as agriculture, demonstrates a need to better understand the differences in modeled distributions and well as model-reanalysis biases.

Conclusions

We have explored the distribution and projected evolution of fire weather in five boreal forest regions covering Alaska, Canada, Siberia, and Fennoscandia. Out analysis provides a systematic characterization of temperature (SAT, SAT_{max}), precipitation, humidity (RH_{min}), wind, as well as the aggregate fire weather index (FWI), under 1850–1900 conditions and for levels of global warming from +1 °C to +4 °C above 1850–1900. By quantifying the full, seasonal probability distribution functions of daily data, we provide more comprehensive information about the potential future changes than available from the change in mean conditions alone.

In all regions, we find marked changes in daily surface air temperature during summer already at +1 °C global warming over the 1850–1900 baseline, i.e. current conditions, as well as clear further shifts between the +1 °C and +2 °C GWLs. At +4 °C, the mean SAT_{max} is higher by 4 °C–5 °C. These changes represent substantial shifts away from the 1850–1900 distribution. The precipitation PDFs show smaller shifts in mean, with an increase in some regions and decrease in other, but a marked widening towards the upper tail. Due to the high intrinsic variability of precipitation, the distributions for 1850–1900 conditions and different GWLs overlap to a higher degree than for other variables. We also estimate a reduction in average RH_{min} in all regions except Alaska, suggesting a summertime drying despite the increase in precipitation extremes, while the mean and upper tails of the distribution of wind generally decreases. We focus on the summer season but note that similar patterns of change are found during spring and fall with potential influence on the fire season duration. Overall, changes are similar in the CanESM ensemble, although generally of smaller magnitude than those in MPI-ESM-1–2-LR. This is particular the case for RH_{min}, where the bias compared to ERA5 is also highest. Given the sensitivity of the FWI to this variable, we suggest further investigations into these differences are needed.

The aggregate impact of changes in the individual variables is an increase in the mean and upper tail of the distribution of daily FWI, as well as a widening suggesting increased variability. Although all regions are projected to experience an increase in the number of days of moderate-to-high FWI days, changes are largest in Canada, which is also the region with the highest average daily FWI at present.

Our present analysis is limited to the influence of key meteorological conditions on fire risk. A more comprehensive understanding of severity and risk from high-latitude wildfire with global warming require combining weather-related risk with changes in landscape and management, ignition sources and demography. Nevertheless, our analysis contributes to increasing the knowledge basis relevant for adaptation and disaster risk management. Our results also demonstrate that combining statistical descriptions with emulation of Earth System Model information, as done here through quantifying the evolution of PDFs, offers an alternative pathway to resource demanding model runs for rapidly translating science to user-oriented information.

Acknowledgments

The authors declare no conflict of interest. We thank Marit Sandstad and Ane Nordlie Johansen (CICERO) for their assistance. This study was conducted as part of the ACRoBEAR project, a project under the Belmont Forum Collaborative Research Action on Climate, Environment and Health. The authors acknowledge funding from the Research Council of Norway (Grant No. 310648) and the European Union's Horizon 2020 research and innovation programme (Grant Agreement No. 101003826), and support from National Infrastructure for High Performance Computing and Data Storage in Norway (UNINETT) resources (Grant No. NN9188K).

Data availability statement

The data that support the findings of this study will be openly available following an embargo at the following URL/DOI: https://doi.org/10.6084/m9.figshare.20730961. Data will be available from 12 June 2023.

ORCID iDs

Marianne T Lund https://orcid.org/0000-0001-9911-4160
Kalle Nordling https://orcid.org/0000-0003-1824-9659
Bjørn H Samset https://orcid.org/0000-0001-8013-1833

References

Abatzoglou J T, Williams A P and Barbero R 2019 Global emergence of anthropogenic climate change in fire weather indices *Geophys. Res. Lett.* **46** 326–36

Balch J K, Abatzoglou J T, Joseph M B, Koontz M J, Mahood A L, McGlinchy J, Cattau M E and Williams A P 2022 Warming weakens the night-time barrier to global fire *Nature* **602** 442–8

Bogerd L, van der Linden E C, Krikken F and Bintanja R 2020 Climate state dependence of arctic precipitation variability *Journal of Geophysical Research: Atmospheres* **125** e2019JD031772
Chen D *et al* 2021a Framing, Context, and Methods *Climate Change 2021: The Physical Science Basis. Contribution of Working Group I to the Sixth Assessment Report of the Intergovernmental Panel on Climate Change* ed V Masson-Delmotte *et al* (Cambridge: Cambridge University Press) pp 147–286
Chen Y, Romps D M, Seeley J T, Veraverbeke S, Riley W J, Mekonnen Z A and Randerson J T 2021b Future increases in Arctic lightning and fire risk for permafrost carbon *Nat. Clim. Change* **11** 404–10
Collins M *et al* 2013 Long-termClimate Change: Projections, Com mitments and Irreversibility *ClimateChange 2013: The Physical Science Basis. Contribution of Working Group I to theFifth Assessment Report of the Intergovernmental Panel on Climate Change* ed T F Stocker *et al* (Cambridge: Cambridge University Press)
Deser C *et al* 2020 Insights from earth system model initial-condition large ensembles and future prospects *Nat. Clim. Change* **10** 277–86
Doerr S H and Santín C 2016 Global trends in wildfire and its impacts: perceptions versus realities in a changing world *Philosophical Transactions of the Royal Society B: Biological Sciences.* **371** 20150345
Feng L, Smith S J, Braun C, Crippa M, Gidden M J, Hoesly R, Klimont Z, van Marle M, van den Berg M and van der Werf G R 2020 The generation of gridded emissions data for CMIP6 *Geosci. Model Dev.* **13** 461–82
Fischer E M and Knutti R 2016 Observed heavy precipitation increase confirms theory and early models *Nat. Clim. Change* **6** 986–91
Flannigan M D, Krawchuk M A, de Groot W J, Wotton B M and Gowman L M 2009 Implications of changing climate for global wildland fire *International Journal of Wildland Fire.* **18** 483–507
Forster P *et al* 2021 The Earth's Energy Budget, Climate Feedbacks, and Climate Sensitivity *Climate Change 2021: The Physical Science Basis. Contribution of Working Group I to the Sixth Assessment Report of the Intergovernmental Panel on Climate Change* ed V Masson-Delmotte *et al* (Cambridge: Cambridge University Press) pp 923–1054
Giannakopoulos C, Karali A and Cauchy A 2020 Fire danger indicators for Europe from 1970 to 2098 derived from climate projections, version 1.0 *Copernicus Climate Change Service (C3S) Climate Data Store (CDS)*
Hantson S *et al* 2020 Quantitative assessment of fire and vegetation properties in simulations with fire-enabled vegetation models from the Fire Model Intercomparison Project *Geosci. Model Dev.* **13** 3299–318
Hersbach H *et al* 2018 ERA5 hourly data on pressure levels from 1979 to present *Copernicus Climate Change Service (C3S) Climate Data Store (CDS)*
Hersbach H *et al* 2020 The ERA5 global reanalysis *Q. J. R. Meteorolog. Soc.* **146** 1999–2049
Holzworth R H, Brundell J B, McCarthy M P, Jacobson A R, Rodger C J and Anderson T S 2021 Lightning in the arctic *Geophys. Res. Lett.* **48** e2020GL091366
Jolly W M, Cochrane M A, Freeborn P H, Holden Z A, Brown T J, Williamson G J and Bowman D M J S 2015 Climate-induced variations in global wildfire danger from 1979 to 2013 *Nat. Commun.* **6** 7537
Jones M W *et al* 2022 Global and regional trends and drivers of fire under climate change *Rev. Geophys.* **60** e2020RG000726
Jones M W, Smith A, Betts R, Canadell J G, Prentice I C and Le Quéré C 2020 Climate change increases the risk of wildfire *ScienceBrief.*
Kasischke E S and Turetsky M R 2006 Recent changes in the fire regime across the North American boreal region—Spatial and temporal patterns of burning across Canada and Alaska *Geophys. Res. Lett.* **33** L09703
Lee B S, Alexander M E, Hawkes B C, Lynham T J, Stocks B J and Englefield P 2002 Information systems in support of wildland fire management decision making in Canada *Comput. Electron. Agric.* **37** 185–98
Lee J Y *et al* 2021 Global climate: scenario based projections and near-term information *Climate Change 2021: The Physical Science Basis. Contribution of Working Group I to the Sixth Assessment Report of the Intergovernmental Panel on Climate Change* ed V Masson-Delmotte *et al* (Cambridge: Cambridge University Press) pp 553–672
Liu Y, Goodrick S and Heilman W 2014 Wildland fire emissions, carbon, and climate: wildfire–climate interactions *Forest Ecology and Management.* **317** 80–96
Lizundia-Loiola J, Otón G, Ramo R and Chuvieco E 2020 A spatio-temporal active-fire clustering approach for global burned area mapping at 250 m from MODIS data *Remote Sens. Environ.* **236** 111493
Maher N, Milinski S and Ludwig R 2021 Large ensemble climate model simulations: introduction, overview, and future prospects for utilising multiple types of large ensemble *Earth Syst. Dynam.* **12** 401–18
Maher N *et al* 2019 The max planck institute grand ensemble: enabling the exploration of climate system variability *Journal of Advances in Modeling Earth Systems.* **11** 2050–69
Mauritsen T *et al* 2019 Developments in the MPI-M earth system model version 1.2 (MPI-ESM1.2) and its response to increasing CO_2 *Journal of Advances in Modeling Earth Systems.* **11** 998–1038
McCarty J L *et al* 2021 Reviews and syntheses: arctic fire regimes and emissions in the 21st century *Biogeosciences.* **18** 5053–83
McCarty J L, Smith T E L and Turetsky M R 2020 Arctic fires re-emerging *Nat. Geosci.* **13** 658–60
McCrystall M R, Stroeve J, Serreze M, Forbes B C and Screen J A 2021 New climate models reveal faster and larger increases in arctic precipitation than previously projected *Nat. Commun.* **12** 6765
Mölders N 2010 Comparison of canadian forest fire danger rating system and national fire danger rating system fire indices derived from weather research and forecasting (WRF) model data for the June 2005 interior alaska wildfires *Atmos. Res.* **95** 290–306
Mudryk L, Santolaria-Otín M, Krinner G, Ménégoz M, Derksen C, Brutel-Vuilmet C, Brady M and Essery R 2020 Historical Northern Hemisphere snow cover trends and projected changes in the CMIP6 multi-model ensemble *The Cryosphere.* **14** 2495–514
O'Neill B C *et al* 2016 The scenario model intercomparison project (ScenarioMIP) for CMIP6 *Geosci. Model Dev.* **9** 3461–82
Pausas J G and Keeley J E 2019 Wildfires as an ecosystem service *Frontiers in Ecology and the Environment.* **17** 289–95
Reid C E, Brauer M, Johnston F H, Jerrett M, Balmes J R and Elliott C T 2016 Critical Review of health impacts of wildfire smoke exposure *Environ. Health Perspect.* **124** 1334–43
Rocha A V and Shaver G R 2011 Postfire energy exchange in arctic tundra: the importance and climatic implications of burn severity *Global Change Biol.* **17** 2831–41
Samset B H, Stjern C W, Lund M T, Mohr C W, Sand M and Daloz A S 2019 How daily temperature and precipitation distributions evolve with global surface temperature *Earth's Future.* **7** 1323–36
Scholten R C, Jandt R, Miller E A, Rogers B M and Veraverbeke S 2021 Overwintering fires in boreal forests *Nature* **593** 399–404
Screen J A, Deser C and Sun L 2015 Projected changes in regional climate extremes arising from Arctic sea ice loss *Environ. Res. Lett.* **10** 084006
Shaposhnikov D *et al* 2014 Mortality Related to Air Pollution with the Moscow Heat Wave and Wildfire of 2010 *Epidemiology.* **25** 359–64
Swart N C *et al* 2019 The canadian earth system model version 5 (CanESM5.0.3) *Geosci. Model Dev.* **12** 4823–73

Touma D, Stevenson S, Lehner F and Coats S 2021 Human-driven greenhouse gas and aerosol emissions cause distinct regional impacts on extreme fire weather *Nat. Commun.* **12** 212

UNEP Spreading like Wildfire 2022 The Rising Threat of Extraordinary Landscape fires. A UNEP Rapid Response Assessment. (Nairobi). https://unep.org/resources/report/spreading-wildfire-rising-threat-extraordinary-landscape-fires, last accessed June 2023

Vajda A, Venäläinen A, Suomi I, Junila P and Mäkelä H M 2014 Assessment of forest fire danger in a boreal forest environment: description and evaluation of the operational system applied in Finland *Meteorol. Appl.* **21** 879–87

Veraverbeke S, Rogers B M, Goulden M L, Jandt R R, Miller C E, Wiggins E B and Randerson J T 2017 Lightning as a major driver of recent large fire years in North American boreal forests *Nat. Clim. Change* **7** 529–34

Van Wagner C E 1987 *Development and structure of the Canadian Forest Fire Weather Index System. Forestry Technical Report 35, 35 p. Canadian Forestry Service, Headquarters* (Ottawa, Canada: National Capital Region)

Walsh J E, Ballinger T J, Euskirchen E S, Hanna E, Mård J, Overland J E, Tangen H and Vihma T 2020 Extreme weather and climate events in northern areas: A review *Earth Sci. Rev.* **209** 103324

Wang Y, Anderson K R and Suddaby R M 2015 Updated source code for calculating fire danger indices in the canadian forest fire weather index system Information Report NOR-X-425. https://publications.gc.ca/collections/collection_2016/rncan-nrcan/Fo133-1-424-eng.pdf. accessed June 2023

van der Wiel K and Bintanja R 2021 Contribution of climatic changes in mean and variability to monthly temperature and precipitation extremes *Communications Earth & Environment.* **2** 1

Woo S H L, Liu J C, Yue X, Mickley L J and Bell M L 2020 Air pollution from wildfires and human health vulnerability in Alaskan communities under climate change *Environ. Res. Lett.* **15** 094019

Xu W, Scholten R C, Hessilt T D, Liu Y and Veraverbeke S 2022 Overwintering fires rising in eastern Siberia *Environ. Res. Lett.* **17** 045005

York A, Bhatt U S, Gargulinski E, Grabinski Z, Jain P, Soja A J, Thoman R L and Ziel R 2020 Wildland fire in high northern latitudes *Arctic Report Card: Update for 2020* ed R L Thoman *et al* (https://doi.org/10.25923/2gef-3964)

Zelinka M D, Myers T A, McCoy D T, Po-Chedley S, Caldwell P M, Ceppi P, Klein S A and Taylor K E 2020 Causes of higher climate sensitivity in CMIP6 models *Geophys. Res. Lett.* **47** e2019GL085782

Zhuang Y, Fu R, Santer B D, Dickinson R E and Hall A 2021 Quantifying contributions of natural variability and anthropogenic forcings on increased fire weather risk over the western United States *Proc. Natl Acad. Sci.* **118** e2111875118

Ziel R H, Bieniek P A, Bhatt U S, Strader H, Rupp T S and York A 2020 A comparison of fire weather indices with MODIS fire days for the natural regions of Alaska *Forests.* **11** 516

Zou Y, Rasch P J, Wang H, Xie Z and Zhang R 2021 Increasing large wildfires over the western United States linked to diminishing sea ice in the Arctic *Nat. Commun.* **12** 6048